

Finite Element Analysis of Permanent Magnet Synchronous Motors Subjected to Symmetrical Voltage Sags

H. Fallah khoshkar*, A. Doroudi*(C.A.) and M. Mohebbi Asl*

Abstract: This paper studies the effects of symmetrical voltage sags on the operational characteristics of a Permanent Magnet Synchronous Motor (PMSM) by Finite Element Method (FEM). Voltage sags may cause high torque pulsations which can damage the shaft or equipment connected to the motor. By recognizing the critical voltage sags, sags that produce hazardous torque variations could be prevented. Simulations results will be provided and the critical voltage sags are recognized. A simple theoretical analysis will also be presented to obtain a qualitative understanding of the phenomena occurring in PMSM during symmetrical voltage sags.

Keywords: Finite Element Method, Maxwell Software, Power Quality, Synchronous Motors, Torque Pulsations, Transient Analysis, Voltage Sag.

1 Introduction

Permanent Magnet Synchronous Motor (PMSM) is a good choice in so many applications. Replacing excitation winding of rotor with Permanent Magnets (PM) makes these motors more efficient than their excited counterparts. The most important advantages of these motors are high efficiency, high power density, low maintenance cost and low loss [1-3].

During the last years, the power quality has gained a great importance for both customers and utilities [4-5]. Power networks may present many types of disturbances, being the voltage sag the most common type. Voltage sags (dips) are about 80 % of frequent phenomena in power systems. The definition of voltage sag is a transitory reduction (10 % to 90 %) in RMS of supply voltage, which lasts from a half a cycle at power supply frequency to one minute [6-7].

If a PMSM is subjected to voltage sags, severe torque peaks may occur which may cause damage and fatigue of the motor shaft or connected equipment. Also, the voltage sag may cause motor disconnect and shutdown by the action of the under-voltage or over-current protection relays [8]. In some applications, the continuity and smoothness of process is important and shutdown of the machine results in production losses and implying large costs. Riding through voltage sags is one way to avoid these unwanted stops [9-10]. In fact, by changing the settings of the protection devices,

dispensable disconnections can be avoided. In these cases, the torque pulsations severity should be evaluated to recognize the sags that motor can ride through them.

This paper investigates the symmetrical voltage sags consequences on PMSM behavior. A qualitative method called "stator flux trajectory analysis" is also presented to show field parameters and the phenomenon occurring in a PMSM during voltage sags. Critical characteristics of voltage sags are obtained easily by some mathematical equations. Finite Element Method (FEM) is utilized to confirm the theoretical analysis and to simulate the saturation effect on the behavior of permanent magnet synchronous motor subjected to voltage sags. The exact magnitudes of flux and torque oscillation are estimated by the FEM.

2 The Governing Equations

Finite element method is a numerical technique for solving problems with complicated geometries, loadings, and material properties where analytical solutions cannot be applied. The method is considered to be the most accurate tool for obtaining the flux density distribution and waveforms in electrical machines. The basic concept is to model a structure by dividing it into small segments called "Elements", interconnected at points common to two or more elements (nodes). The properties of the elements are formulated as equilibrium equations. The equations for the entire structure are obtained by combining the equilibrium equation of each element such that continuity is ensured at each node. The necessary boundary conditions are then imposed and the equations of equilibrium are solved to find the required variables.

Iranian Journal of Electrical & Electronic Engineering, 2014.

Paper first received 16 Oct. 2013 and in revised form 1 July 2014.

* The Authors are with the Department of Electrical Engineering, Shahed University, Tehran, Iran.

E-mails: Hossein_falah66@yahoo.com, doroudi@shahed.ac.ir and morteza.mohebbi@gmail.com.

The governing equation on a PMSM is [11-12]:

$$\sigma \frac{\partial A}{\partial t} - \left(\frac{1}{\mu_0}\right) \nabla^2 A - \sigma v \times (\nabla \times A) = -\sigma \nabla \phi + \nabla \times M \quad (1)$$

where σ is the electrical conductivity, μ_0 is the magnetic permeability of free space, v is the velocity of the material with respect to a given reference frame, and M is the magnetization vector. A is magnetic vector potential and ϕ is electric scalar potential that their relationships with other field variables are given as follows:

$$B = \nabla \times A \quad (2)$$

$$E + \frac{\partial A}{\partial t} = -\nabla \phi \quad (3)$$

where B is magnetic flux density and E is electric field intensity.

To avoid the velocity term in the above equation, a Lagrangian coordinate system is used, in which the variables are fixed to the materials and hence the velocity is always zero. Also, given the assumption of two-dimensional analysis, the problem can be reduced to scalar form and the magnetic vector potential A is reduced to the z-axis scalar A_z :

$$\sigma \frac{\partial A_z}{\partial t} - \left(\frac{1}{\mu_0}\right) \nabla^2 A_z = -\sigma \nabla \phi + \nabla \times M \quad (4)$$

Eq. (4) is the basic governing equation for the problem that should be solved by FEM.

3 Finite Element Analysis

A 4-pole, 1.5 kW line-operated permanent magnet synchronous motor is modeled using Maxwell software. The 2D motor structure and main dimensions and the finite element mesh generated are shown in Fig. 1 and the motor ratings and parameters are given in appendix.

Due to symmetry, the study of the whole machine structure can be reduced to a study only one of the pole of the motor (One quarter of the structure). This yields the double advantages:

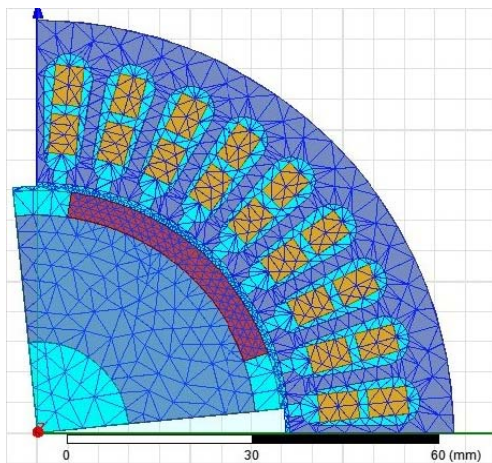


Fig. 1 PMSM structure and main dimensions.

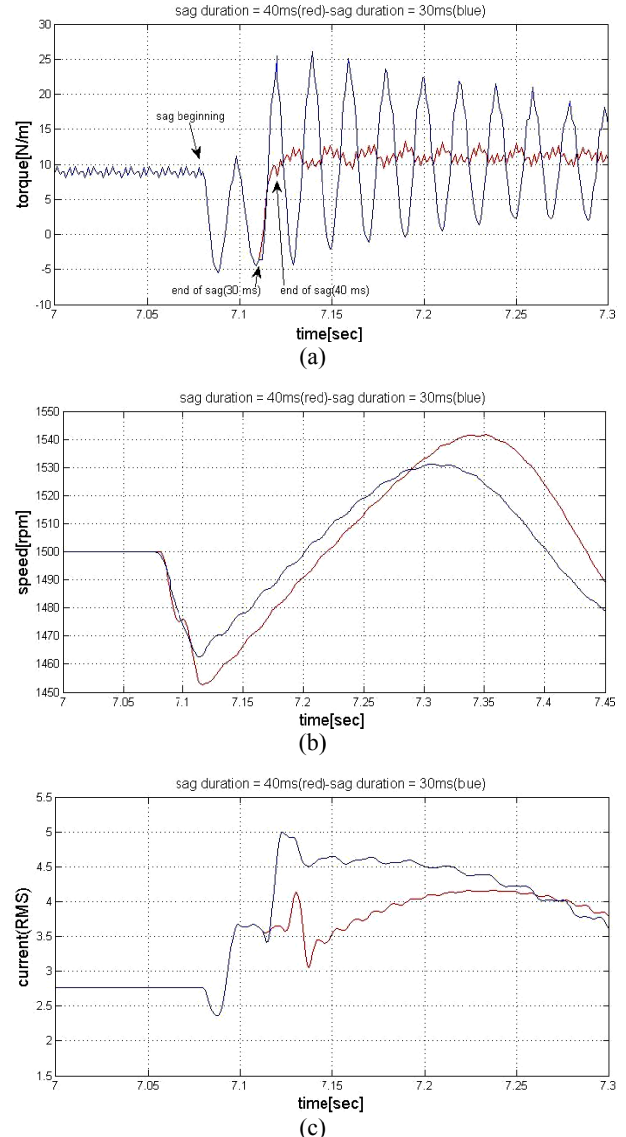


Fig. 2 a) Torque b) speed c) phase current of PMSM versus time-sag depth $h = 0.3$, sag durations: 1.5 and 2 cycles.

- The reduction of the domain to be analyzed, with the resultant reduction of the calculation time.
- The possibility of a more accurate analysis of the remaining part by increasing the number of meshes in that part.

Before voltage sag and at the steady state conditions, the motor draws one per unit real power in nominal terminal voltage and at unity power factor. A constant-power mechanical load has been assumed in the simulation. It is assumed that at the instant when the sag begins, the voltage of phase a is expressed by:

$$v_a(t) = V_m \cos(\omega t + \theta_0) \quad (5)$$

The other phases should modify by ± 120 shifting. θ_0 is the voltage phase angle at the sag beginning instant (initial point of wave). It is assumed that voltage sags have a rectangular shape. Rectangular voltage sag is a

momentary voltage drop to a fixed level in the RMS value and immediately restoration of the voltage level to the pre sag voltage level (1.0 pu) sometime later. This shape is very often used in simulations as it is very simple to use and it represents the worst case [13-14]. Symmetrical three phase voltage sag of magnitude h has been considered. In this paper, sag magnitude, h , is the net root mean square (rms) voltage in percentage or per unit of system rated voltage.

Fig. 2 shows torque, speed and phase current variations, before, during and after two voltage sags of amplitude $h = 0.3$ and durations of 1.5 and 2 cycles

occurring at the motor terminal. The voltage sag begins at the time $t = 7.08$ sec. The initial point of voltage wave is assumed -78° .

As it is seen from Fig. 2, there are two important instants where the severity of torque pulsations may be large: at the sag beginning and at the instant of voltage restoration. The post sag peak torque has a high value for the sag duration 1.5 cycles while it has a relatively smaller value for the sag duration of 2 cycles. The pattern of speed changes is opposite to that of torque variations due to assumption of constant power mechanical load.

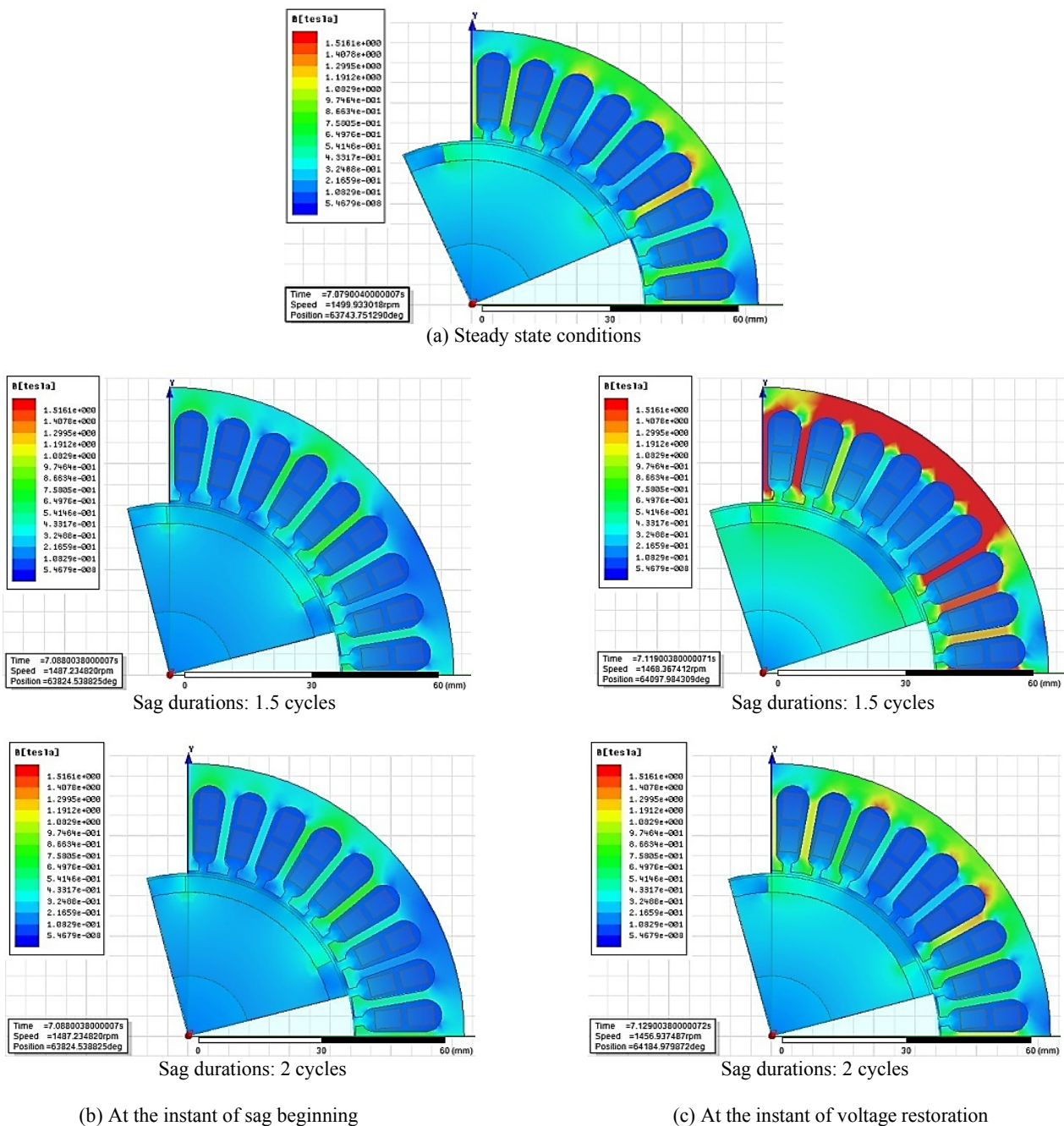


Fig. 3 Flux density distribution at (a): steady state conditions and at the instants of (b): sag beginning and (c): voltage restoration – sag depth $h=0.3$, sag durations: 1.5 and 2 cycles.

On the other hand, the pattern of the variations of the peaks of the phase current with the sag durations is similar to that of the change of the peaks of the post sag air-gap torque.

Fig. 3 shows the flux density distribution in the motor at the steady state conditions and at the instants of torque peaks occurring ($h = 0.3$, sag duration = 1.5 and 2 cycles). The figure depicts that at the instant of voltage restoration, the stator flux density is approximately the same as steady state condition flux density when duration of voltage sag is 2 cycles. On the other hand, the maximum of flux density has reached to 2.78 T which is approximately as two times as much as in steady state when duration of voltage sag is 1.5 cycles. Obviously, in real machines, the flux cannot reach to this level due to saturation.

Several simulations were carried out by the FEM and the followings are the simulations results:

- Deeper voltage sags causes in general larger torque peaks.
- The torque peak at the sag beginning does not depend to the θ_0 (the initial point of wave). It depends only to the sag magnitude. In the other words, for the symmetrical sags, the initial point-on-wave has no influence on the torque peak at the beginning on the sag.
- The torque peak at the end of the sag depends to the duration of the sag. If the sag duration is a multiple of the period time of the supply, the lowest additional transients would occur. If the sag duration is a multiple of the period time of the supply plus half, the biggest torque peak would occur. In fact, the change of this peak with the sag duration is oscillatory with a frequency equal to the supply frequency (50 Hz). The peak value also changes as a function of the sag magnitude.

4 Stator Flux Trajectory Analyses: Simple Theoretical Approach

In this section, a simplified theoretical analysis is performed to obtain a qualitative understanding of the phenomena occurring in PMSM during symmetrical sags. In the analysis, the flux variations are calculated in a complex plain (with d and q as axes) using the voltage sag equations. For simplicity, the stator resistance and saturation are neglected and the rotor speed is assumed constant during the entire duration of the sag.

By applying Park transformation [15], symmetrical voltage sag equations will be as follows:

$$\begin{aligned} V_q &= hV_m \cos \theta_0 \\ V_d &= hV_m \sin \theta_0 \\ V_0 &= 0 \end{aligned} \quad (6)$$

Prior to the sag and in a complex plain with d and q axes as coordinates, the internal voltage of the machine in the synchronous reference frame can be expressed as:

$$E_s = jV_m e^{j(\theta_0 + \delta)} \quad (7)$$

The synchronous reference frame is assumed to lead the stator reference frame by an angle γ . Consequently, the internal voltage of the machine in the stator reference frame is given by:

$$E_s^s = jV_m e^{j(\theta_0 + \delta)} e^{j(\omega t + \gamma)} \quad (8)$$

where superscript s denotes stator reference frame. The modulus of the stator flux linkage prior to the sag is $\psi_{s0} = V_m/\omega$. The stator flux in stator reference frame is thus expressed as:

$$\begin{aligned} \psi_s^s &= \psi_d^s + j\psi_q^s \\ &= \psi_{s0} e^{j(\delta + \gamma)} e^{j(\omega t + \theta_0)} \end{aligned} \quad (9)$$

It is assumed that the sag occurs at $t = 0$. Then the initial fluxes in the synchronous and stator reference frames are:

$$\psi_{s(t=0)} = \frac{V_m}{\omega} e^{j(\delta + \theta_0)} \quad (10)$$

$$\psi_{s(t=0)}^s = \frac{V_m}{\omega} e^{j(\delta + \theta_0 + \gamma)} \quad (11)$$

During the sag, the internal voltage of the machine can be given by:

$$E_{s(dur.sag)}^s = jhV_m e^{j(\theta_0 + \delta)} e^{j(\omega t + \gamma)} \quad (12)$$

The change in the flux can be obtained by integration of voltage wave:

$$\begin{aligned} \Delta \psi_{s(dur.sag)}^s &= \int_0^t E_s^s dt \\ &= \frac{hV_m}{\omega} e^{j(\theta_0 + \delta + \gamma)} (e^{j\omega t} - 1) \end{aligned} \quad (13)$$

The resulting flux is thus obtained by adding the change to the initial value. This results is as:

$$\psi_{s(dur.sag)}^s = \frac{V_m}{\omega} e^{j(\theta_0 + \delta + \gamma)} (1 - s) + \frac{hV_m}{\omega} e^{j(\theta_0 + \delta + \gamma)} e^{j\omega t} \quad (14)$$

To find the stator flux in the synchronous reference frame, the transformation coefficient $e^{-j(\omega t + \gamma)}$ can be used:

$$\psi_{s(dur.sag)} = \frac{V_m}{\omega} e^{j(\theta_0 + \delta)} \left(h + (1 - h) e^{-j\omega t} \right) \quad (15)$$

Eq. (15) is described by a constant term and a rotating term in negative direction. The constant term multiplied by h which shows the average value of flux reduces during the sag. The rotating term causes flux changes in d - q axes coordination.

According to Eq. (15) and for specified values of θ_0 and δ , the flux path during the sag will follow a circle and moves one turn in each cycle. The starting point is initial flux point. The centre of the circle is the point that if the sag duration lasts enough, the flux will finally reach to this point ($\psi_{s(t=\infty)} = h\psi_{s(t=0)}$). The radius of the circle initially will be the distance between initial flux and $\psi_{s(t=\infty)}$ named as ρ_d^A , and then reduces with armature time constant. During the sag, the severity of torque

pulsations depends on this radius. The bigger radius of the circle, the more severe the torque pulsations.

$$\rho_d^A = \frac{V_m}{\omega}(1-h) \quad (16)$$

Note that radius of the circle only depends on h and is independent of θ_0 and δ . Fig. 4(a) shows the flux path (dotted line) calculated by FEM for $h = 0.3$, $\theta_0 = -78^\circ$ and $\delta = 30^\circ$. Duration of the sag is assumed 2 cycles. Note that the exponential decay of the modulus is not predicted by the simplified theory as we neglected the stator resistance.

When the voltage restores, which is set by the duration of the voltage sag, the flux at each point where exists, tends to back to the initial point. Again, the flux will point along a new circle. The larger the distance between flux at the instant of voltage restoration and the initial flux, the bigger the new circle radius and the more severe the torque pulsations.

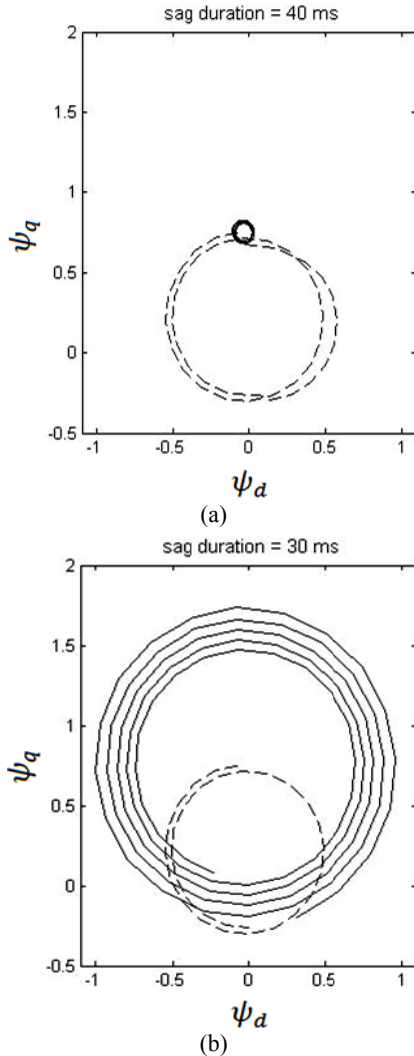


Fig. 4 Stator flux in complex coordination in the synchronous reference frame during and after symmetrical sag of amplitude $h=0.3$ and duration (a):2 and (b): 1.5 cycles.

If the duration of voltage sag is a multiple of the period-time of the supply ($\omega t = 2k\pi$ where k is an integer), the stator flux will be:

$$\psi_s^s = \frac{V_m}{\omega} e^{j(\theta_0 + \delta + \gamma)} \quad (17)$$

which is the same as the initial flux. This means that no additional transients would occur if the voltage was restored at that instant. Fig. 4(a) shows stator flux (solid line) in the synchronous reference frame after a symmetrical voltage sag occurring. As expected, after voltage restoration, the flux pointed along a new circle. Since the sag duration is a multiple of the period-time of the supply, at the voltage restoration instant, the flux is near to its initial position and hence, the torque peak will be minimum.

On the other hand, if the duration of the voltage sag is assumed α plus any number of full periods, we would have:

$$\psi_{s(t=t_{sag})}^s = \frac{V_m}{\omega}(1-h + h e^{j(\alpha + 2k\pi)}) \quad (18)$$

When the voltage is restored, the internal voltage of the motor will be given by:

$$E_s^s = j V_m e^{j(\theta_0 + \delta)} e^{j(\omega t + \gamma)} \quad (19)$$

The flux change is thus equal to:

$$\begin{aligned} \Delta \psi_{s(after\ sag)}^s &= \int_{t=\frac{\alpha}{\omega}}^t E_s^s dt \\ &= \frac{V_m}{\omega} e^{j(\theta_0 + \delta + \gamma)} (e^{j\omega t} - e^{j\alpha}) \end{aligned} \quad (20)$$

Then the resultant flux is:

$$\psi_{s(after\ sag)}^s = \frac{V_m}{\omega} e^{j(\theta_0 + \delta + \gamma)} [(1-h)(1 - e^{j\alpha}) + 1] \quad (21)$$

Performing the transformation in the synchronous reference frame yields:

$$\psi_{s(after\ sag)}^s = \frac{V_m}{\omega} e^{j(\theta_0 + \delta)} [1 + (1-h)(1 - e^{j\alpha}) e^{-j\omega t}] \quad (22)$$

This equation is similar to the expression for the stator flux during the sag in Eq. (15). An important difference is the rotating term amplitude which is equal to the new circle radius ρ_r^A :

$$\rho_r^A = |(1-h)(1 - e^{j\alpha})| = 2(1-h) \sin \frac{\alpha}{2} \quad (23)$$

The point correspond to the maximum value of ρ_r^A i.e. $\alpha = 2k\pi + \pi$, produces the most severe torque pulsations (called critical symmetrical sag). In this situation, the flux at the ending of the sag has the maximum distance from the initial value and the torque peak after the voltage restoration will be maximum. Fig. 4(b) shows the flux path in this situation calculated by FEM. As it is seen, the new circle radius is larger than ρ_d^A .

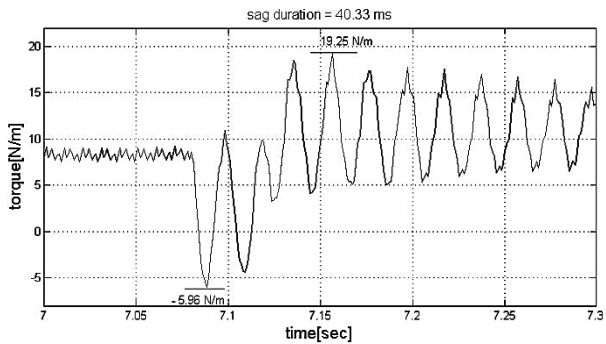


Fig. 5 Torque variations versus time ($h=0.3$, sag duration=2.167 cycles).

One other interesting case is $\alpha = 2k\pi + \pi/3$. In this condition $\rho_d^A = \rho_r^A$ that means the severity of torque pulsations at the sag beginning and ending are equal. Fig. 5 shows the torque variations at this situation calculated by FEM.

5 Saturation Effects

In the analysis of the transient performance of PMSM during and after voltage sags, the accurate calculation of the motor behavior depends on the saturation condition [16]. Let us consider the Eq. (22) again. It is obvious that the rotating term of the stator flux has twice the amplitude after voltage restoration while $\alpha = 2k\pi + \pi$ and $h = 0$. Adding this to steady state value, stator flux might be theoretically three times as much as in steady state. Obviously, in real machines, the flux cannot reach to this level due to the saturation.

In order to study the saturation effects on the operational characteristics of the PMSM, the model in Eq. (1) has been implemented by FEM again. The difference is that saturation is included by taking into accounts B-H curve of steel_1008 lamination for stator of PMSM. In the analysis of electrical machines, the problem becomes nonlinear due to the presence of ferromagnetic materials. The permeability is a function of the local magnetic field, which unknown at the start of the problem. In this case we must use an iterative process and keep correcting the permeability until it is consistent with the field solution. The most popular method of dealing with nonlinear problems in magnetic is the Newton-Raphson method [17]. Fig. 6 shows the flux density distribution of the PMSM at the instant of voltage restoration where $h = 0.3$, sag duration is 1.5 cycles and saturation is included. The figure can be compared with Fig. 3(c) which shows the unsaturated model. As it can be seen, there is a significant decrease in the calculated flux density. Fig. 7 shows the motor phase current with and without saturation included. The figure depicts that the phase current is higher when saturation is included. Fig. 8 shows torque variations versus time with and without saturation included. As it is seen from this figure, there is not so much effect on

the torque due to saturation. This is as a result of this fact that the torque is the product of flux and current and if the flux is reduced due to saturation, the current is increased, so the product is almost the same.

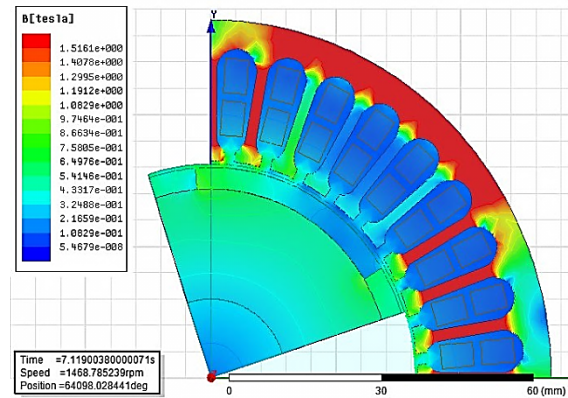


Fig. 6 Flux density distribution at the instants of voltage restoration-sag depth $h=0.3$, sag durations: 1.5- saturation included.

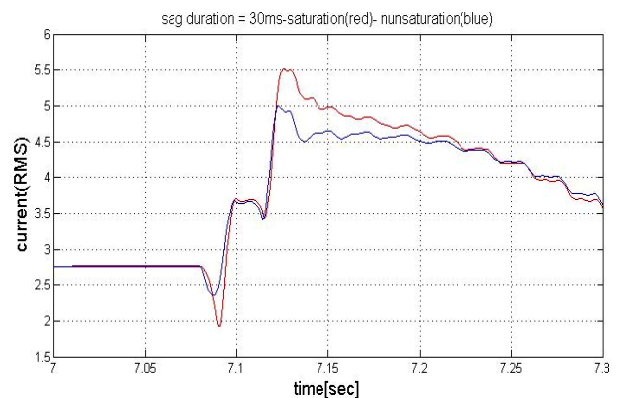


Fig. 7 phase current of PMSM versus time – sag depth $h = 0.3$, sag durations: 1.5 cycles- with (red color) and without (blue color) saturation.

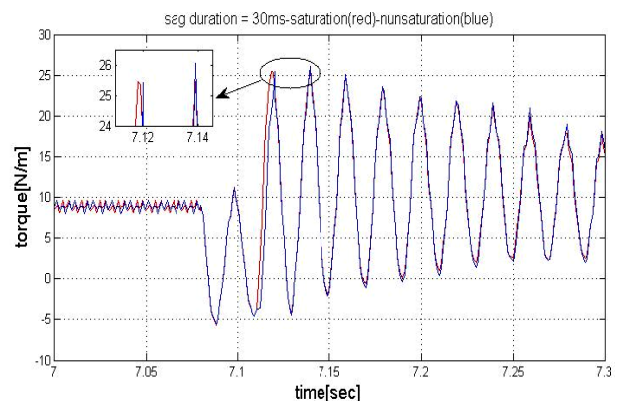


Fig. 8 Torque versus time – sag depth $h = 0.3$, sag durations: 1.5 cycles- with (red color) and without (blue color) saturation.

6 Conclusion

A simplified theoretical analysis is presented to investigate the effects of voltage sags on PMSM torque pulsations at the beginning and end of the sags. The method can specify the most unfavorable conditions during and at the ending instant of the symmetrical voltage sag. The torque peak at the beginning on the sag only depends on the sag depth and the initial point-on-wave has no influence on it. The duration of the voltage sag is as important as the depth of the sag for the peak torque and current at the ending of the sag. The worst peak torque occurs for $h = 0$ with a duration of half a period plus any full periods.

FEM is utilized to confirm the theoretical analysis and to simulate the saturation effect on the behavior of permanent magnet synchronous motor subjected to voltage sags. The results show that voltage sag may cause saturation in the motor. Saturation causes significant decrease in the flux density and increase in the phase current but there is not so much effect on the torque peaks.

Appendix

Table 1 Data of designed PM synchronous motor.

Quantity	Value
Input frequency	50 Hz
Input voltage (line-to-line)	295.0 V
Connection	Y
Inner diameter of the stator	82.5 mm
Outer diameter of the stator	136.0 mm
Air gap in d axis (clearance)	0.3 mm
Air gap in q axis (clearance)	5.4 mm
Effective length of the stator core	103.0 mm
Stacking factor for the stator core	0.96
Armature winding coil pitch	64.8 mm
Length of a single overhang	90.8 mm
Number of turns per phase	240
Number of parallel conductors	2
Number of stator slots	36
Stator wire conductivity at 20° C	$57 * 10^{-6}$ S/m
Diameter of stator conductor	0.5 mm
Width of the stator slot opening	2.2 mm
Height of permanent magnet	5.0 mm
Width of permanent magnet	3*10 mm
Length of permanent magnet	100.0 mm
Permanent magnetic flux density	1.0 T
Coercive force	700.0 kA/m
Width of pole shoe	32.4 mm
Thickness of pole shoe	1.0 mm

References

[1] A. Jabbari, M. Shakeri and S. A. Nabavi Niaki, "Pole Shape Optimization of Permanent magnet synchronous motors Using the Reduced Basis

Technique", *Iranian Journal of Electrical and Electronic Engineering*, Vol. 6, No. 1, pp. 48-55, 2010.

- [2] M. J. Soleimani Keshayeh and S. Asghar Gholamian, "Optimum Design of a Three-Phase Permanent Magnet Synchronous Motor for industrial applications", *Int. Journal of Applied Operational Research*, Vol. 2, No. 4, pp. 67-86, 2013.
- [3] C. Lucas, Z. Nasiri-Gheidari and F. Tootoonchian, "Using Modular Pole for Multi-Objective Design Optimization of a Linear Permanent magnet synchronous motor by Particle Swarm Optimization (PSO)", *Iranian Journal of Electrical and Electronic Engineering*, Vol. 6, No. 4, pp. 214-223, 2010.
- [4] J. Beiza, S.H. Hosseinian and B. Vahidi, "Fault Type Estimation in Power Systems", *Iranian Journal of Electrical and Electronic Engineering*, Vol. 5, No. 3, pp. 185-195, 2009.
- [5] M. Aliakbar-Golkar and, Y. Raisee-Gahrooyi, "Stochastic Assessment of Voltage Sags in Distribution Networks", *Iranian Journal of Electrical and Electronic Engineering*, Vol. 4, No. 4, pp. 191-201, 2008.
- [6] M. H. J. Bollen, *Understanding Power Quality Problems*, IEEE Press, 2000.
- [7] R. C. Dugan, M. F. McGranaghan and S. Santoso, *Electrical Power systems Quality*, McGraw-Hill, 2004.
- [8] F. Carlsson, P. Nee and C. Sadarangani, "Analysis of Peak Torque of Line-Operated Synchronous Machines Subjected to Symmetrical Voltage Sags", *Power Electronics Machines and Derives Conference Publication*, pp. 480-485, 2002.
- [9] L. Guasch, F. Corcoles and J. Pedra, "Effects of Symmetrical and Unsymmetrical Voltage sags on Induction Machines", *IEEE Trans. on Power Delivery*, Vol. 19, No. 2, pp. 774-782, 2004.
- [10] D. Aguilar, A. Luna, A. Rolan, C. Vazquez and G. Acevedo, "Modeling and simulation of Synchronous Machine and its Behavior against Voltage sags", *IEEE Int. Symposium on Industrial Electronics (ISIE)*, pp. 729-733, 2009.
- [11] S. J. Salon, *Finite Element Analysis of Electrical Machines*, Kluwer Academic Publishers, 1995.
- [12] C. C. Hwang and Y. H. Cho, "Effects of Leakage Flux on magnetic Fields on Interior Permanent Magnet Synchronous Motors", *IEEE Trans. on Magnetics*, Vol. 37, No. 4, pp. 3021-3024, 2001.
- [13] D. Aguilar, A. Luna, A. Rolan, C. Vazquez and G. Acevedo, "Symmetrical and Unsymmetrical Voltage sag effects in the Three-phase Synchronous Machine Stability", *13th European Conference on Power Electronics and Applications*, pp. 1-7, 2009.

- [14] J. Alipoor, A. Doroudi and M. Ghaseminezhad, "Detection of the Critical Duration of Different Types of Voltage Sags for Synchronous Machine Torque Oscillation", *Energy and Power Engineering (EPE)*, Vol. 4, No. 3, pp. 117-124, 2012.
- [15] P. C. Krause, O. Wasynczuk and S. D. Sudhoff, *Analysis of Electric Machinery and Drive Systems*, Wiley-IEEE Press, 2002.
- [16] N. C. Kar and A. M. El-Serafi, "Effect of Voltage Sag on the Transient Performance of Saturated Synchronous Motors", *IEEE CCECE/CCGEI*, pp. 1246-1251, 2006.
- [17] S. J. Salon, *Finite Element analysis of Electrical Machines*, Kluwer academic publishers, 1995.



Hossein Fallah khoshkar was born in Tehran, Iran, in 1987. He received the B.Sc. degree from the Electrical Eng. Dept. of Azad University, saveh, Iran, in 2010 and the M.Sc. degree in electrical engineering from Shahed University, Tehran, Iran, in 2013. His especial fields of interest include power converter circuits and Power Quality.



Aref Doroudi was born in 1968 in Tehran, Iran. He received the B.Sc. degree from the Electrical Eng. Dept. of Amirkabir University of technology, Tehran, Iran, in 1992 and the M.Sc. degree in electrical engineering from Tabriz University, Tabriz, Iran, in 1994 and Ph.D. degree in Electrical Engineering Dept, of Amirkabir University of technology, Tehran, Iran, in 2000. At the present, he is the assistant Professor of Electrical engineering Department in Shahed University, Tehran, Iran. His especial fields of interest include Power Quality, Electric Machines Design and power systems dynamic.



Morteza Mohebbi Asl was born in Tehran, Iran in 1981. He received the B.Sc. degree from Khaj-e Nasir-e Toosi University and M.Sc. degree from Iran University of Science & Technology in control engineering in 2003 and 2006, respectively. Presently he is Ph.D. student in Shahed University, Tehran, Iran. His research covers fault localization in power transformers.